Scientific Journal of Engineering & Pharmaceutical Science (https://damaacademia.com/sjeps/)
Volume 1, Issue 5, pp.27-47, May 2019
Published by: Dama Academic Scholarly & Scientific Research Society (www.damaacademia.com)

Modelling of Electric Fields in High-Voltage X-Ray Devices

[1]Nancy Ma | Eric J. Miller | Vincent F. Jones | Kris J. Kozaczek
Moxtek, Inc., 452 W 1260 N, Orem, UT 84057
Email: nma@moxtek.com

Abstract
During the operation of a high-voltage x-ray device, high voltage stresses increase risk of dielectric breakdown. It is critically important that these systems are designed so that the magnitude of the electric field or the electric field stress are within the material limits for dielectric breakdown. In the present investigation, a simplified x-ray device is numerically modelled for two limiting cases with sharp edges and with perfectly-rounded edges to understand the numerical behavior of these solutions and to determine optimal geometry for minimizing electric field stress.
Keywords: *Electric Field Singularities; Electric Field Stress; Electrostatics; High Voltage; Numerical Modelling; X-Ray*

1.0 INTRODUCTION

X-rays are commonly used for analytical applications such as x-ray spectrometry and spectroscopy, destructive testing, as well as imaging in 2D and 3D applications such as medical, dental, and veterinary imaging [1]. In all these applications, the recent trend is to miniaturize the instrumentation which means that there are substantial development efforts to reduce the size and weight of x-ray generating devices. The handheld devices, such as x-ray fluorescence for atomic composition measurements, backscatter imaging for security applications, dental imaging or fluoroscopic inspection, require that the x-ray tube and the high voltage power supply be packaged as one unit, called an x-ray source, in order to reduce the size and weight, and to simplify the integration in the final product. All hand-held x-ray instruments operate in the range of 35 kV to 160 kV. For high-voltage applications, design and simulation are challenging due to large gradients which cause arcing and dielectric breakdown [2,3]. This, in turn, can result in large gradients of the electric field, or the electric field stress. This is an especially challenging issue in miniature x-ray sources for portable devices [4]. Efficient numerical modelling of electrostatics is key to quantifying this electric field stress and designing systems that do not exceed dielectric breakdown limits. Iterative test and build is very time intensive and costly in materials and human resources. Numerical codes can be developed using finite element methods, finite difference methods or spectral methods [5-8]. Industrial applications have complex geometries and complex physical phenomena that require high-fidelity commercial codes to provide accurate predictions. ANSYS Maxwell is a state-of-the-art low-frequency and static solver for electromagnetics. ANSYS Maxwell offers a finite-element approach that utilizes an adaptive meshing algorithm [9]. This is the tool of choice for the present investigation.

Every dielectric material has a rating for electrical or dielectric breakdown or dielectric strength. If the magnitude of the electric field, or electric field stress, exceeds the material's dielectric breakdown limit, the material turns from a dielectric material to an electrically-conducting material. In a given part, the electric field stress must everywhere be less than this breakdown limit. This is an especially important issue in high-voltage devices for hand-held applications [10,11]. Very large values of the electric field stress can cause undesirable electric arcing which can produce unwanted heat, electric current flow and electrical energy that vaporizes the material. Failure frequently has undesirable coupled consequences thermally, mechanically, hydrodynamically and chemically [12]. This can be fatal for high-voltage devices resulting in complete operational failure. At a sharp corner or edge between a dielectric and an electrical conductor, the equipotential lines are sharp and the derivative of the electric potential can become mathematically infinite. Since the electric field is the negative of the gradient of the electric potential, this implies mathematically that the electric field is also infinite. This is referred to as an electric field singularity. Classen *et al.* [13] and McCoy [14] propose integral approaches to eliminate electric field singularities at sharp corners and edges.

This paper investigates the effect of the geometry on the electric field stress in an x-ray device. In the original system, there are sharp edges on the chassis package. As the mesh density increases, the electric field stress increases without bound, because the numerical solutions more accurately capture the mathematically infinite behavior. This paper investigates two different approaches, which are (a) the geometry with a sharp edge, in which the solution is valid outside a certain distance from the singularity, and (b) a geometric approach in which the geometry is rounded to mitigate the risk of a sharp corner or edge. Results are discussed for these two cases.

2.0 Problem Formulation

This paper treats the static electric potential in an x-ray device in order to understand the effect of the geometrical shapes and the special arrangement of the high-voltage power supply on the electric fields. Figure 1 shows a simplified schematic of the essential components of the x-ray source, which are an x-ray tube, a printed circuit board with high voltage multiplier and controls, and a high-voltage feedback resistor, which are all enclosed in a chassis. In this fundamental study, the geometry has been greatly simplified to focus on the region between the resistor and the protrusion of the chassis into the isolator, containing sharp edges. This protruding sheet metal is used for mounting the printed circuit boards.

Therefore, the x-ray tube is approximated as a single cylinder, only one printed circuit board with simplified geometry is included, one resistor with simplified geometry is included, and all other electronic components are neglected. The x-ray tube is sealed and held at high vacuum. The remainder of the volume inside the chassis is filled with silicon-polymer-based potting material. The purpose of this investigation is to understand the electrostatic behavior in the region between the resistor and the knife edge, as well as variations in the geometry of the knife edge. The chassis is made of aluminum, the resistor is modelled as copper, the printed circuit board is made of FR4 and the potting is made of Sylgard 185. For Sylgard 185, the dielectric permittivity is 2.68 [15]. The overall footprint is 3.19" by 4.83", and the height at the front of the component is 3.68". This corresponds to 8.10 cm by 12.27 cm, and a height of 9.35 cm.

Maxwell's equations are a set of four linear partial-differential equations which represent the coupled behavior of the electric potentials and electric currents to both applied and induced magnetic and electric fields [16,17]. The steady form of Maxwell's equations are

$$\nabla \times \mathbf{H} = \mathbf{j} \qquad (1a)$$

$$\nabla \cdot \mathbf{B} = 0 \qquad (1b)$$

$$\nabla \times \mathbf{E} = 0 \qquad (1c)$$

$$\nabla \cdot \mathbf{D} = \rho_e \qquad (1d)$$

where **j** is the electric current density, **H** is the magnetic field, **D** is the displacement field, **B** is the magnetic flux density or magnetic intensity, and ρ_e is the charge density. Equations (1a), (1b), (1c) and (1d) are Ampere's Law, Gauss' Law for Magnetism, Maxwell-Faraday Law, and Gauss' Law for Electricity, respectively.
The electromagnetic constitutive equation which relates electric field and displacement field is

$$\mathbf{D} = \varepsilon_d \mathbf{E} \qquad (2)$$

where ε_d is the material's dielectric permittivity. The electric field is related to voltage or electric potential ϕ by

$$\mathbf{E} = -\nabla\phi \, . \qquad (3)$$

For the present electrostatic problem, there is no applied magnetic field and any induced magnetic fields or electric currents are negligible. For a material with isotropic dielectric permittivity, substituting Eqs. (2) and (3) into Gauss' Law (1d) yields the differential equation governing electric potential

$$\varepsilon_d \nabla^2 \phi + \rho_e = 0 \, . (4)$$

The electric potential must satisfy the Maxwell-Faraday Law given by Eq. (1c). Substituting Eq. (2) into Eq. (1c) yields

$$\nabla \times \nabla \phi = 0 \, . \qquad (5)$$

The chassis' parts shown in Fig. 1 are grounded at 0 V. An excitation or voltage of -60,000 V is applied to the high-voltage feedback resistor. These voltage excitations are applied uniformly to these parts' volumes so that the voltage is spatially uniform and the electric fields are identically equal to zero inside these parts. In the present situation where excitations are applied in the form of electric potential or voltage, Eq. (4) has two unknowns, which are electric potential ϕ and charge density ρ_e. Inside an electrical conductor, the electric field is equal to zero and there is no

numerical solution in the volume of a conductor. In the presence of an externally-applied electric field, the free charges in the dielectric materials redistribute, yielding a spatial distribution of the charge density ρ_e.
The magnitude of the electric field |**E**| is given by

$$|\mathbf{E}| = \sqrt{E_x^2 + E_y^2 + E_z^2} \qquad (6)$$

where E_x, E_y and E_z are the components of the electric field in the Cartesian coordinate system. This is also referred to as the electric field stress.

The differential equations (4) and (5), which govern the electric potential and charge density, can be solved by various numerical methods. In the present investigation, ANSYS Maxwell, a finite-element based solver, is used to solve for the voltage distribution and quantify the electric field magnitude given by Eq. (6). Some import studies have modelled the electrostatics using finite element methods in other important applications [18,19]. Sima *et al*. [18] investigated the behavior of the electric field in ice while Cui *et al*. [19] investigated electric fields in high-voltage power lines. ANSYS Maxwell is a state-of-the-art electromagnetic simulation software which can be utilized to solve static problems. ANSYS Maxwell provides high-fidelity numerical solutions based on the finite element method using an adaptive mesh generation algorithm. The computational domain is discretized, meaning it is subdivided into a number of small volumes called finite elements. The finite elements are connected to its neighbors through vertices or nodes and through their boundaries.

The system of partial differential equations which govern the underlying physics are applied to these small volumes, which yields a system of linear algebraic equations that govern the variables at the nodes. This system of equations can then be solved by either direct or iterative methods. For the current three-dimensional electrostatics simulation, there are two degrees of freedom for the scalar quantities electric potential and charge density. The simulation time is proportional to $(2N)^3$, where N is the number of nodes in the finite element mesh. The dependence of the accuracy of the solution is systematically investigated as the number of node or elements is increased. The mesh is refined until an acceptable error is achieved. For electrostatics, a system's potential energy, U, is given by

$$U = \iiint \mathbf{E} \bullet \mathbf{D}\, dV \quad (7)$$

This potential energy, also called electric potential energy or electrostatic potential energy, represents the work required to bring the system to the given electric state. For a system with applied excitations, this electric potential energy is a known quantity. ANSYS Maxwell calculates this value based on the input excitations and compares the finite element solution to this value for each iteration. For electrostatics, ANSYS Maxwell uses adaptive meshing which refines the mesh based on the solution meeting user-specified criteria. The user specifies the maximum number of iterations and maximum tolerable error. The adaptive meshing undergoes an iterative procedure in which an initial mesh is generated and a solution is calculated. At each iteration, the solver evaluates three criteria, which are (a) whether the user-specified number of iterations has been exceeded, (b) whether the maximum tolerable error is less than the error for electric potential energy, and (c) whether the maximum tolerable error is less than the error between the present iteration and the previous iteration.

3.0 Results and Discussion

The present investigation is focused on the region with the largest electric potential gradient, which is in the potting between the resistor and the knife edge part of the chassis. The potting material is a dielectric while the chassis is an electrical conductor. Results are discussed for two cases. The first case includes the 90° edge on all edges of the chassis, as shown in Fig. 1. When sheet metal is formed, unfortunately, the chassis or housing automatically has these sharp edges. Metal surface treatment can be used to chemically dissolve sharp edges and corners. This surface preparation technique can be implemented by soaking the chassis in a light acid solution. The second case considers a chassis in which the edges are removed by a light acid solution, effectively creating a radius in place of a machined knife edge. This is an excellent alternative to retaining the sharp edge because this is relatively simple and inexpensive to implement. This also has the benefit of removing burrs created by machining operations.

3.1 Sharp Knife Edge

For the first case, the chassis' edges are sharp with 90° edges, as shown in Fig. 1. The user-specified error criterion or allowable error was systematically decreased from 1% to 0.003% in order to understand the effect of the

number of elements on the solution. For the mesh refinement study, three results were monitored, which are (i) the peak magnitude of the electric field at the knife edge, (ii) the peak magnitude of the electric field at the resistor, and (iii) the magnitude of the electric field on a line extending from the knife edge to the resistor. In Fig. 2, a top view of the x-ray device shows this line extending from the knife edge to the resistor.

For 1% maximum allowable error, the adaptive mesh refinement algorithm terminated with an actual error of 0.64% and with a mesh having 17,687 tetrahedral elements. For this coarse mesh, the peak value of the electric field magnitude at the knife edge was 102 V/mil. For 0.1% maximum allowable error, the adaptive mesh refinement algorithm terminated with an actual error of 0.08% and with a mesh having 29,900 tetrahedral elements, which represents a 69% increase. The peak electric field magnitude at the knife edge increased by 26% to 129 V/mil. For 0.04% maximum allowable error, the adaptive mesh refinement algorithm terminated with an actual error of 0.015% and with a mesh having 50,535 elements, which represents a 69% increase. The peak electric field magnitude at the knife edge increased by 31% to 168 V/mil. For a 0.02% maximum allowable error, the adaptive mesh refinement algorithm terminated with an actual error of 0.0106% and with a mesh having 85,415 elements, which represents a 69% increase. The peak electric field magnitude at the knife edge continued to increase substantially to a value of 201 V/mil. The peak electric field magnitude at the knife edge continues to increase due to the sharp edge. The electric field magnitude around the resistor is converging with a relatively constant value as the mesh is continually refined.

The maximum tolerable error was continually decreased to a value of 0.003%, for which the mesh had 1,990,304 elements. For this mesh, the solution converged with an error of 0.002327%. The peak electric field magnitude continued to increase due to the sharp knife edge, as shown in Fig. 3. In Figs. 4a through 4e, results are shown for electric potential and electric field for the most accurate result, with 0.002327% actual error having 1,990,304 elements. Figure 4a presents the equipotential lines on a horizontal plane just above the chassis' knife edge. This plane lies parallel to the printed circuit board below the tube and cuts through the resistor. In Fig. 4a, the surface of the resistor has a value of -60,000 V and the values increase with distance away from the resistor until they reach a maximum value of 0 V at the grounded knife edge. In Fig. 4b, the contours of the electric field magnitude just above the surface of the chassis' knife edge are presented. The peak value of 876 V/mil occurs on the knife edge where the curve in the edge transition into a straight line extending towards the back of the device. Unfortunately, this is not a mesh-independent solution due to the sharp edge, and this value continues to increase with mesh density as shown in Fig. 3.

In a plane normal to that shown in Figs. 4a and 4b, the equipotential lines are presented in Fig. 4c. This plane includes the line shown in Fig. 2, so that the scoped results are skewed relative to the device's global coordinate system. The surface of the resistor has an electric potential of -60,000 V and the potential increases with distance from the resistor until a maximum value of 0 V is reached. In Fig. 4d, the contours of the electric field magnitude are presented in this same plane. In Fig. 4e, the electric field magnitude is presented along the line extending between the knife edge and the resistor shown in Fig. 2. There are four curves shown for maximum allowable error of 1%, 0.1%, 0.04% and 0.003%. As the error is decreased and the mesh density is correspondingly increased, the electric field magnitude at the knife edge continually increases. As the mesh density increases, the finite element solution is concentrating more elements at the knife edge's sharp edge. This results in a more accurate numerical solution at the edge, which more accurately captures the electric field singularity or mathematically infinite behavior. For the maximum allowable error of 0.003%, the electric field magnitude is 876 V/mil. In Fig. 4e, the peak value for the vertical (ordinate) axis has been truncated at 600 V/mil for convenience, so this value of 876 V/mil is not shown in the chart. These results exhibit the singular behavior that occurs at sharp interfaces between dielectrics and electrical conductors.

At some distance away from the knife edge, perhaps about 0.05", the values of the electric field magnitude exhibit the typical convergence behavior as the mesh density increases. The values away from the knife edge are considered converged with a maximum allowable error of 0.04% or actual error of 0.08%. The solution in the domain outside of 0.05" is considered valid. Within this distance from the singularity, the solution is non-convergent and the results are not quantitative. This distance is highly dependent on the specific geometry and excitations. Unfortunately, the peak value of the electric field magnitude for a sharp edge is not directly quantifiable. There may be ways to utilize criteria to define acceptable limits such as the cumulative stress method [20] and the Weidmann criteria [21] but these would need to be tested and validated.

3.2 Rounded Knife Edge

A straightforward and cost effective approach to mitigating or eliminating unpredictable risk with a sharp knife edge is to round the knife edge. In the solid model in Fig. 1a, the chassis is made of sheet metal having thickness 0.03". Submerging the chassis into a light acid solution can chemically dissolve sharp edges and burrs. With the

sharp edges rounded by a light acid solution, fillets with radius 0.015" are assumed, as shown in Fig. 5. The sheet metal's thickness and fillets correspond to dimensions of 0.0762 cm and 0.0381 cm, respectively. For the limiting case of a sharp edge at an interface between a dielectric and an electrical conductor, the equipotential lines are sharp and the derivative of the electric potential is mathematically infinite. When the edge is rounded with a small radius of curvature, the equipotential lines are continuous but the gradient of the electric potential, or the electric field, is still very large. As the radius of curvature increases, the spacing and curvature of the equipotential lines become more uniform and, thus, the electric field magnitude decreases. For the present rounded knife edge, the fillet radius is half the chassis' thickness so that its cross section is semi-circular. Therefore, the knife edge is perfectly rounded and the electric field stress is minimized.

The user-specified error criterion or maximum allowable error was systematically decreased in order to understand the behavior of the solution and obtain an accurate converged mesh-independent result. For the mesh refinement study, three results were monitored, which are (i) the peak magnitude of the electric field at the knife edge, (ii) the peak magnitude of the electric field at the resistor, and (iii) the magnitude of the electric field on a line extending from the knife edge to the resistor. The same line shown in Fig. 2 was utilized. For a maximum allowable error of 1%, the adaptive mesh algorithm terminated at an error of 0.93642% with a mesh having 21,684 elements. For this mesh, the peak electric field magnitude at the knife edge was 308 V/mil while the peak electric field magnitude at the resistor was 1,436 V/mil. When the mesh was further refined with a maximum allowable error of 0.1%, the adaptive mesh algorithm terminated at 0.068646% with a meshing having 36,659 elements, which is a 69% increase from the initial mesh. The peak electric field magnitude at the knife edge decreased 33% to 206 V/mil while this value at the resistor decreased 29% to 1,013 V/mil.

Further decrease in error or increase in the mesh density resulted in less than a 3% change in the solution. This is reflected in Fig. 6 which shows the peak values of the electric field magnitude at the knife edge and resistor versus number of elements. Figure 6 shows that the solution converged quickly and remained relatively constant as the number of elements increased after the initial refinement. For comparison, the curve for the sharp knife edge is included in Fig. 6, demonstrating the difference in the convergence behavior with and without the sharp edge. For the finest mesh considered, the solution adaptive mesh algorithm terminated with an error of 0.002387% with a mesh having 1,877,217 elements. For this mesh, the peak value of the electric field magnitude at the knife edge is 224 V/mil. With the present material assumptions, both the resistor and the knife edge are excellent electrical conductors. The electric field magnitudes were generally higher adjacent to the resistor, because the resistor has a smaller radius than the radius of curvature of the knife edge. The equipotential lines around the resistor are more concentrated, resulting in a higher electric potential gradient or electric field. If the resistor had been modelled with the coating and dielectric material, then the electric field stress would be far lower around the resistor.

In the horizontal plane just above the knife edge, Figures 7a and 7b present the contours of the electric potential and electric field magnitude. In Fig. 7b, the peak value of the electric field magnitude converged at a value of 224 V/mil. Due to the rounded knife edge, the solution is mathematically finite and the electrostatic solver was able to converge to a solution as the mesh density was increased. Figure 7c presents the electric field magnitude versus the distance from the knife edge along the line extending from the knife edge to the resistor shown in Figs. 2a and 2b for maximum allowable errors of 1% and 0.003%. With the rounded knife edge, the peak electric field magnitude is bounded at the knife edge with a peak value of 224 V/mil. The singular behavior with the sharp knife edge is no longer occurring. With the rounded knife edge, the singularity that exists at a sharp edge between a dielectric and an electrical conductor has been eliminated. The results demonstrate the typical convergence behavior in which the error decreases as the mesh density increases.

4.0 Conclusions

The singular behavior along the sharp knife edge has been demonstrated with progressively increasing values of the electric field magnitude as the mesh density or number of elements increases. This behavior exists at sharp corners and edges between dielectrics and electrical conductors. For a rounded knife edge, this mathematically infinite behavior disappeared and the solution was bounded and convergent. The results with the rounded knife edge demonstrated the typical numerical behavior where the solution asymptotes to a converged solution as the mesh density is increased.

For a mesh with 10,000 elements, the ratio between the electric field magnitude for the sharp edge and for the rounded edge is 5.5. Because the sharp edge is singular, this ratio increases as the mesh density increases. Numerical modelling has proven to be a very useful tool in predicting electrical standoff, which allows for designing with appropriate margins to reduce overall size and weight.

Nomenclature

B Magnetic flux density (T)
D Displacement field (C/m^2)
E Electric field (V/m or V/mil)
j Electric current density (A/m^2)
H Magnetic field (A/m)
N Number of nodes
U Electric potential energy or energy stored in an electric field (J)
V Volume (m^3)

Greek Symbols

ε_p Dielectric permittivity (F/m)
φ Electric potential (V)
μ_p Magnetic permeability (H/m)
ρ_e Charge density (C/m^3)
σ Electrical conductivity (S/m)

References

[1] J. T. Bushberg, J. A. Seibert, E. M. Leidholdt and J. M. Boone, *The Essential Physics of Medical Imaging*, Lippincott, Williams & Wilkins, 2012.
[2] W. G. Dunbar, High Voltage Design Guide: Aircraft, Aero Propulsion Laboratory, Air Force Wright Aeronautical Laboratories, AFWAL-TR-82-2057, 1983.
[3] M. S. Naidu and V. Kamaraju, High Voltage Engineering, The McGraw-Hill Companies, New York, 2009.
[4] E. Miller, S. Cornaby, G. Smith, R. Steck, B. Harris, K. Kozaczek and S. Kamtekar, "120-kV and 5-Watt compact x-ray source," SPIE Proceedings of Advances in Laboratory-Based X-Ray Sources, Optics and Applications VI, Vol. 10387, 2017.
[5] Z. Qiao, Z. Li and T. Tang, "A finite difference scheme for solving the nonlinear Poisson-Boltzmann equation modeling charged spheres," *Journal of Computational Mathematics*, Vol. 24, pp. 252-264, 2006.
[6] N. Ma and J. S. Walker, "Strong-field electromagnetic stirring in the vertical gradient freeze process with a submerged heater," *Journal of Crystal Growth*, Vol. 291, pp. 249-257, 2006.
[7] X. Wang, N. Ma, D. F. Bliss and G. W. Iseler, "Solute segregation during modified vertical gradient freezing of alloyed compound semiconductor crystals with magnetic and electric fields," *International Journal of Heat and Mass Transfer*, Vol. 49, no. 19/20, pp. 3429-3438, 2006.
[8] Y. Y. Khine, R. M. Banish and J. I. D. Alexander, "Convective contamination in self-diffusivity experiments with an applied magnetic field," *Journal of Crystal Growth*, Vol. 250, pp. 274-278, 2003.
[9] "Maxwell Online Help," Release 18.2, ANSYS Inc., 2017.
[10] S. Cornaby and K. Kozaczek, "X-Ray Sources for Handheld X-Ray Fluorescence Instruments," *Encyclopedia of Analytical Chemistry*, John Wiley & Sons, 2016.
[11] S. Cornaby, A. Reyes-Mena, H. K. Pew, P. W. Moody, T. Hughes, A. Stradling, D. C. Turner and L. V. Knight, "An XRD/XRF instrument for the microanalysis of rocks and minerals," *Materials Science & Technology*, Vol. 12, pp. 676-683, 2001.
[12] J. K. Nelson, "An assessment of the physical basis for the application of design criteria for dielectric structures," IEEE Transactions on Electrical Insulation. Vol. 24, pp. 835-847, 1989.
[13] C. Classen, E. Gjonaj, U. Römer, R. Schuhmann and T. Weiland, "Modeling of field singularities at dielectric edges using grid based methods," *Advances in Radio Science*, Vol. 9, pp. 39-44, 2011.
[14] P. A. McCoy, "Electromagnetic field singularities," *Journal of Mathematical Analysis and Applications*, Vol. 275, No. 2, pp. 761-770, 2002.
[15] Sylgard 184 Silicone Elastomer Technical Data Sheet, The Dow Chemical Company, Form No. 11-3184B-01 C, 2014.
[16] Fano, R. M., L. J. Chu and R. A. Adler, *Electromagnetic Fields, Energy and Forces*, John Wiley & Sons, New York, New York, 1960.
[17] Katsenelenbaum, B. Z., *High-Frequency Electrodynamics*, John Wiley & Sons, 2006.
[18] W. Sima, Q. Yang, C. Sun and F. Guo, "Potential and electric-field calculation along an ice-covered composite insulator with finite-element method," IEEE Proceedings of Generation, Transmission and Distribution, Vol. 153, pp. 343-349, 2006.

[19] Y. Cui, H. Yuan, X. Song, L. Zhao, Y. Liu and L. Lin, "Model, design and testing of field mill sensors for measuring electric fields under high-voltage direct-current power lines," IEE Transactions on Industrial Electronics, Vol. 65, pp. 608-615, 2018.
[20] J. K. Nelson, "An assessment of the physical basis for the application of design criteria for dielectric structures," *IEEE Transactions of Electrical Insulation*, Vol. 24, pp. 835-847, 1989.
[21] R. Schultz, "Creepage Withstand Strength of Transformerboard," WICOR Insulation Conference, Rapperswil, Switzerland, 1996.

List of Figures

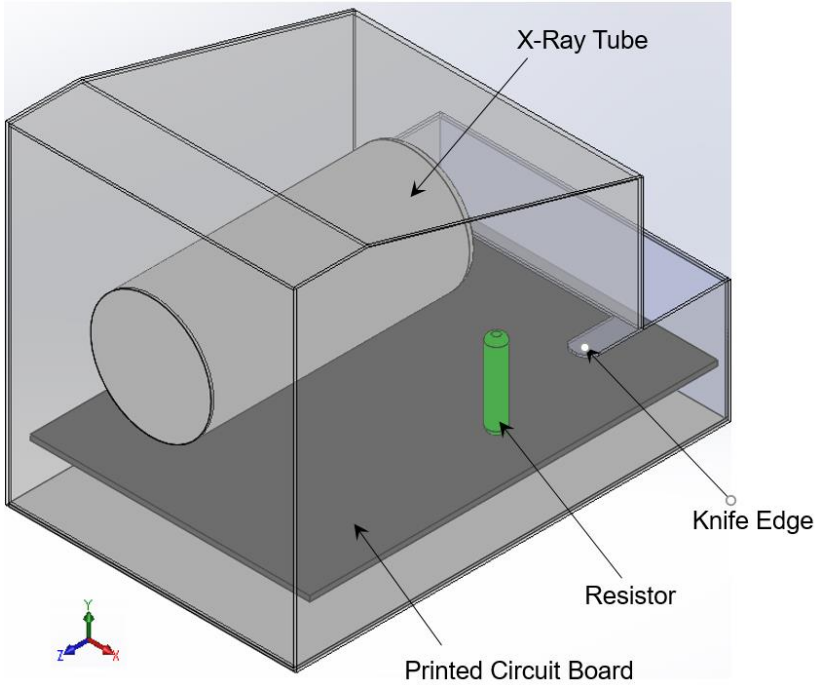

Figure 1

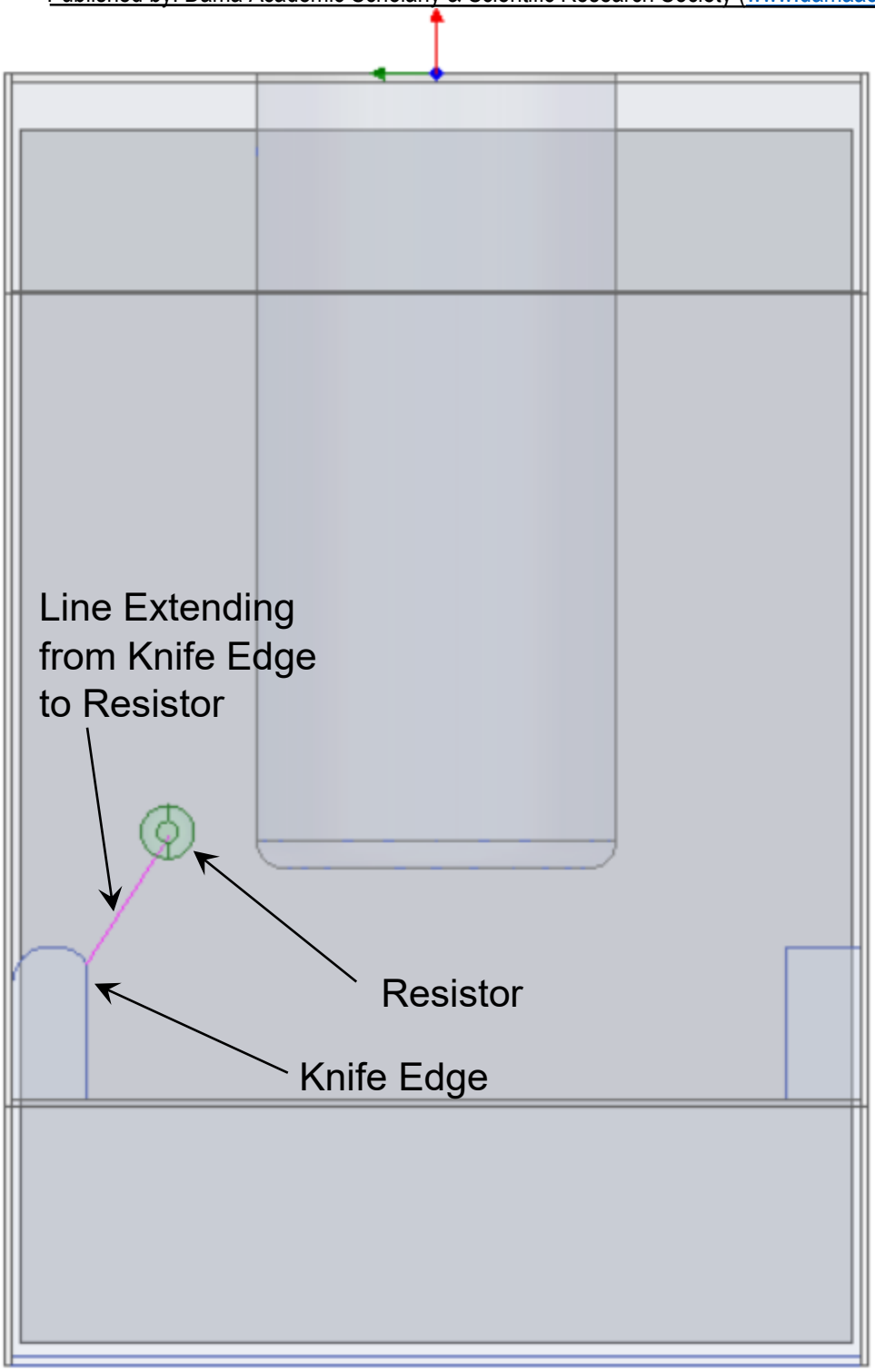
Line Extending
from Knife Edge
to Resistor
Resistor
Knife Edge

Figure 2a

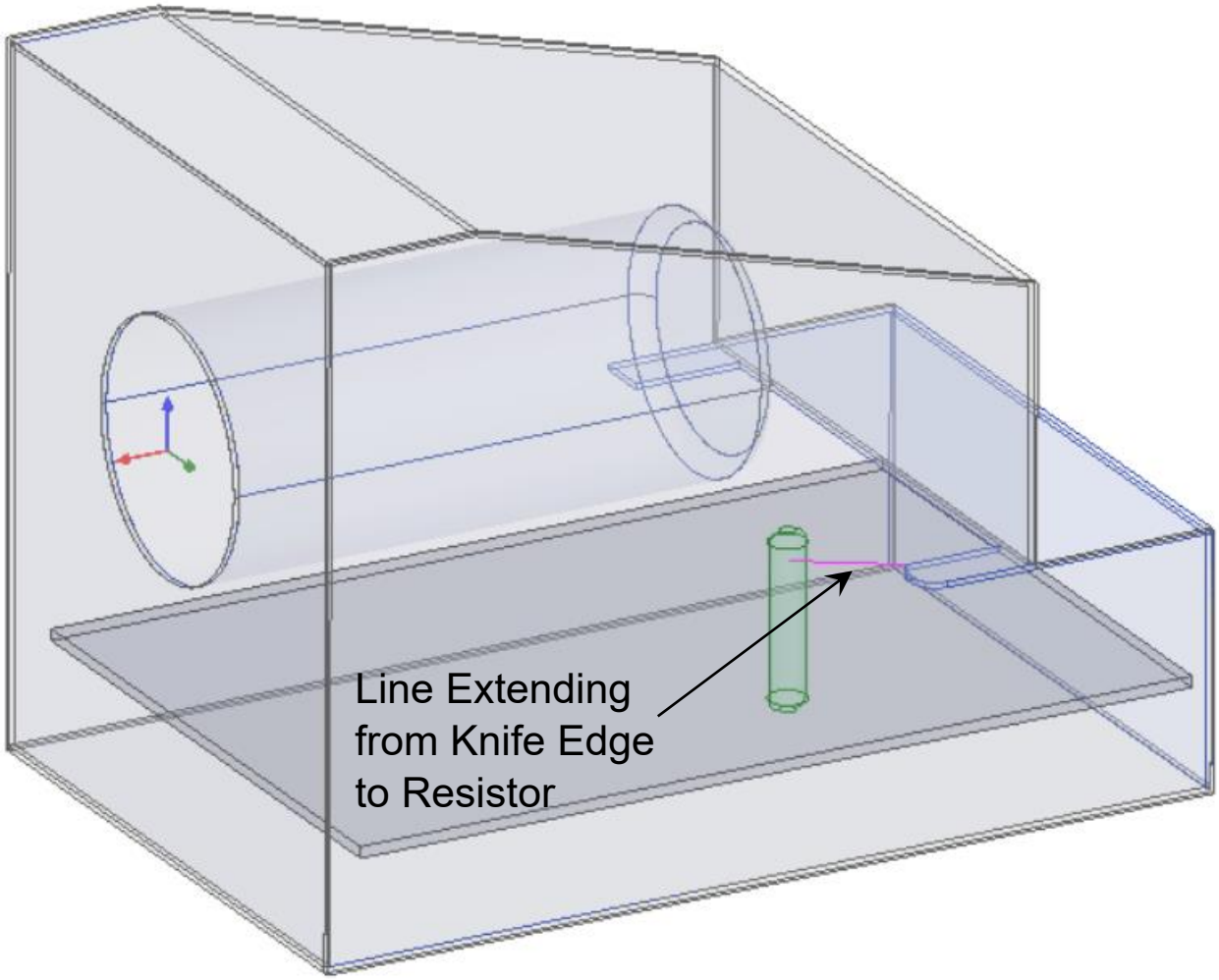

Figure 2b

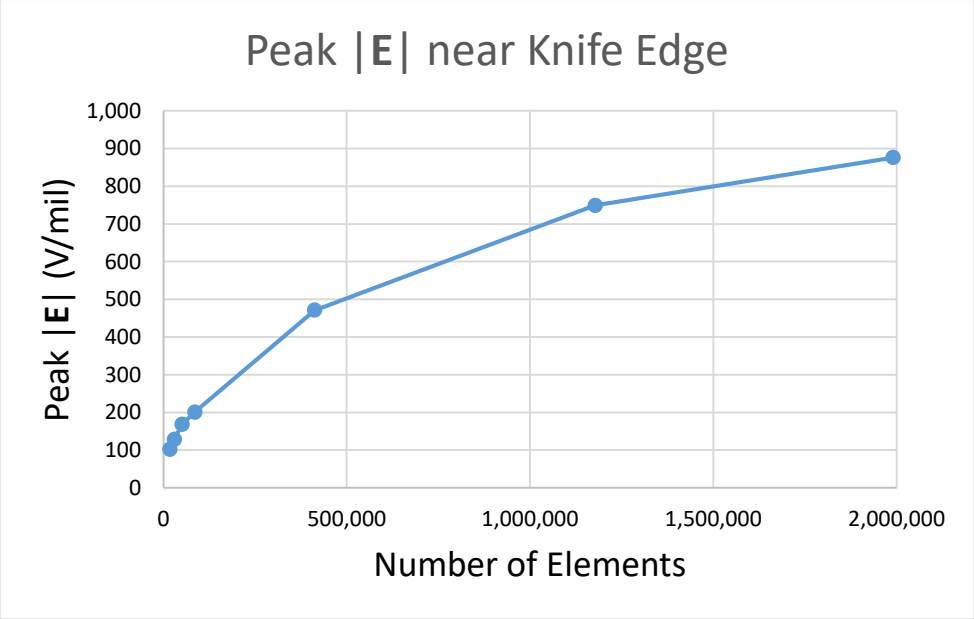
Peak |E| near Knife Edge
Peak |E| (V/mil)
1,000
900
800
700
600
500
400
300
200
100
0
0
500,000
1,000,000
1,500,000
2,000,000
Number of Elements

Figure 3

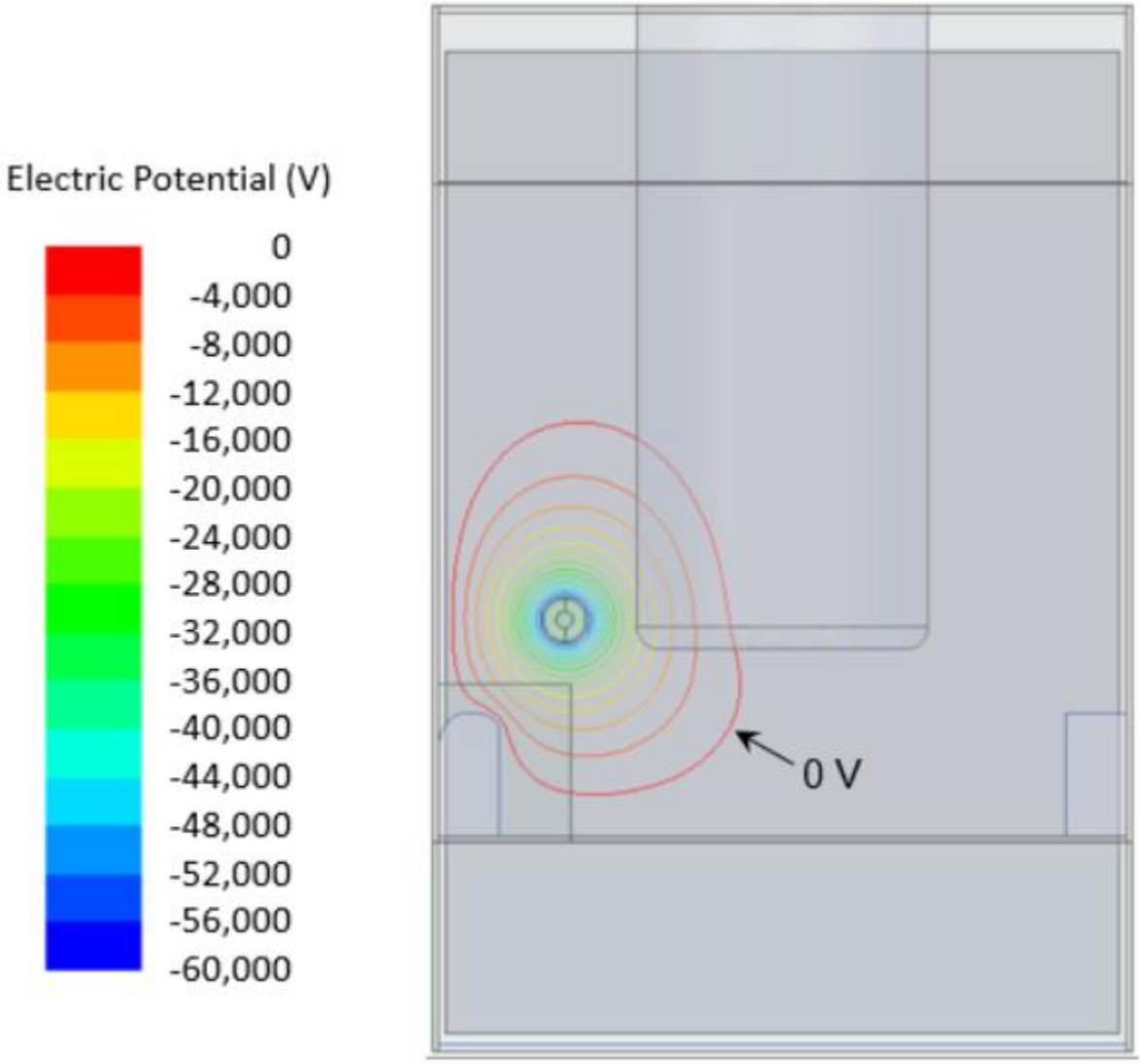

Figure 4a
Please use color for this figure in print.

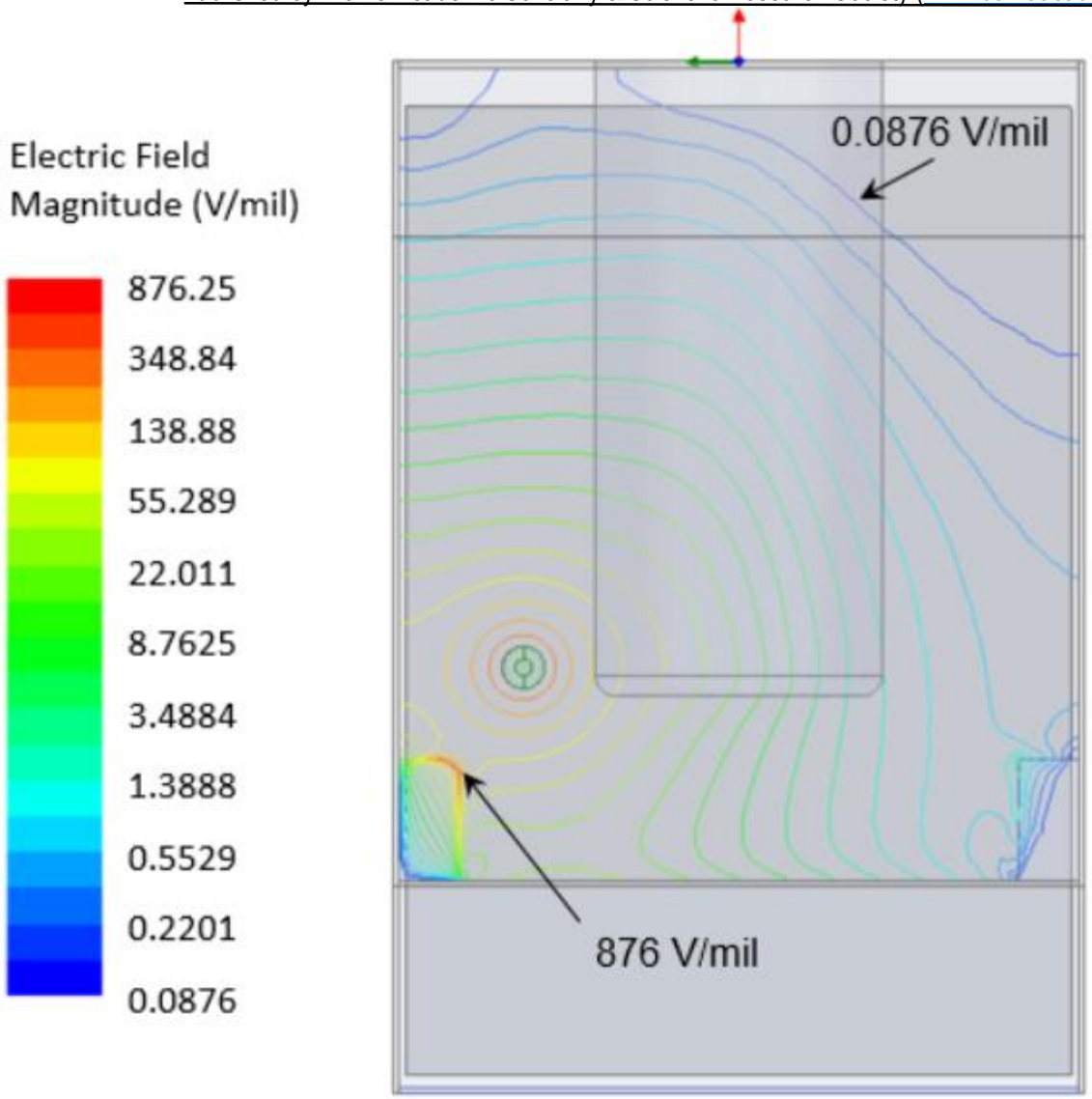

Figure 4b
Please use color for this figure in print.

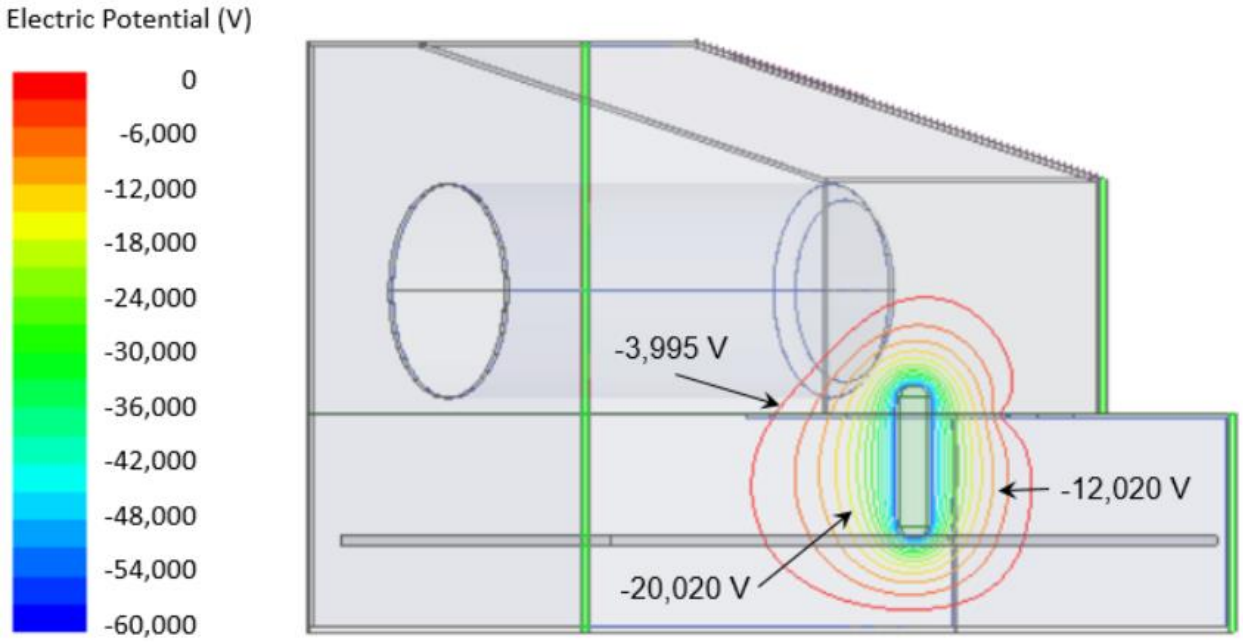

Figure 4c
Please use color for this figure in print.

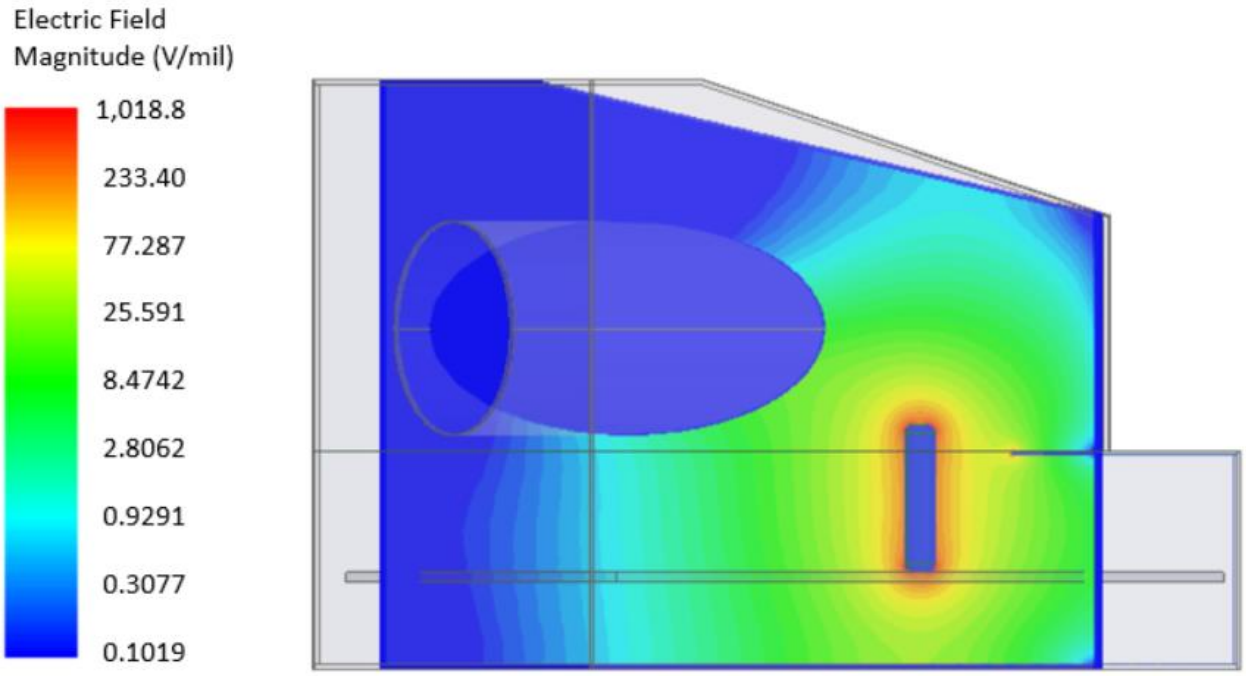

Figure 4d
Please use color for this figure in print.

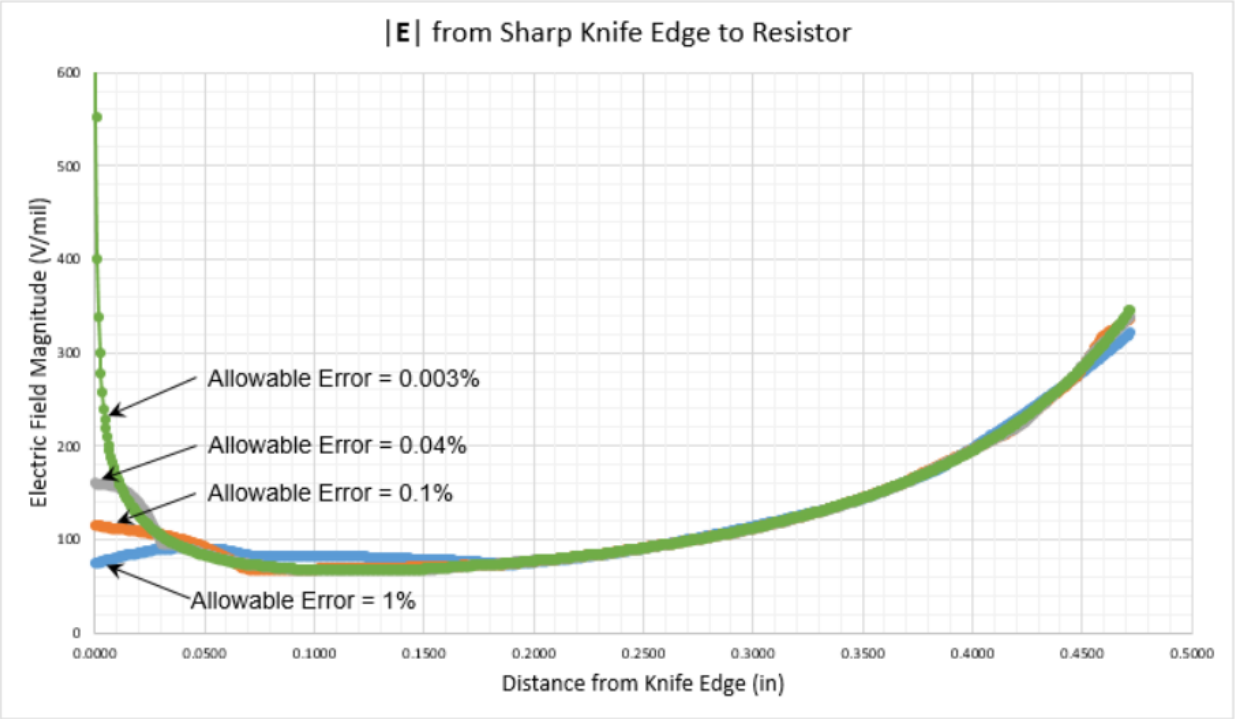
|E| from Sharp Knife Edge to Resistor
Electric Field Magnitude (V/mil)
600
500
400
300
200
100
0
Allowable Error = 0.003%
Allowable Error = 0.04%
Allowable Error = 0.1%
Allowable Error = 1%
0.0000
0.0500
0.1000
0.1500
0.2000
0.2500
0.3000
0.3500
0.4000
0.4500
0.5000
Distance from Knife Edge (in)

Figure 4e

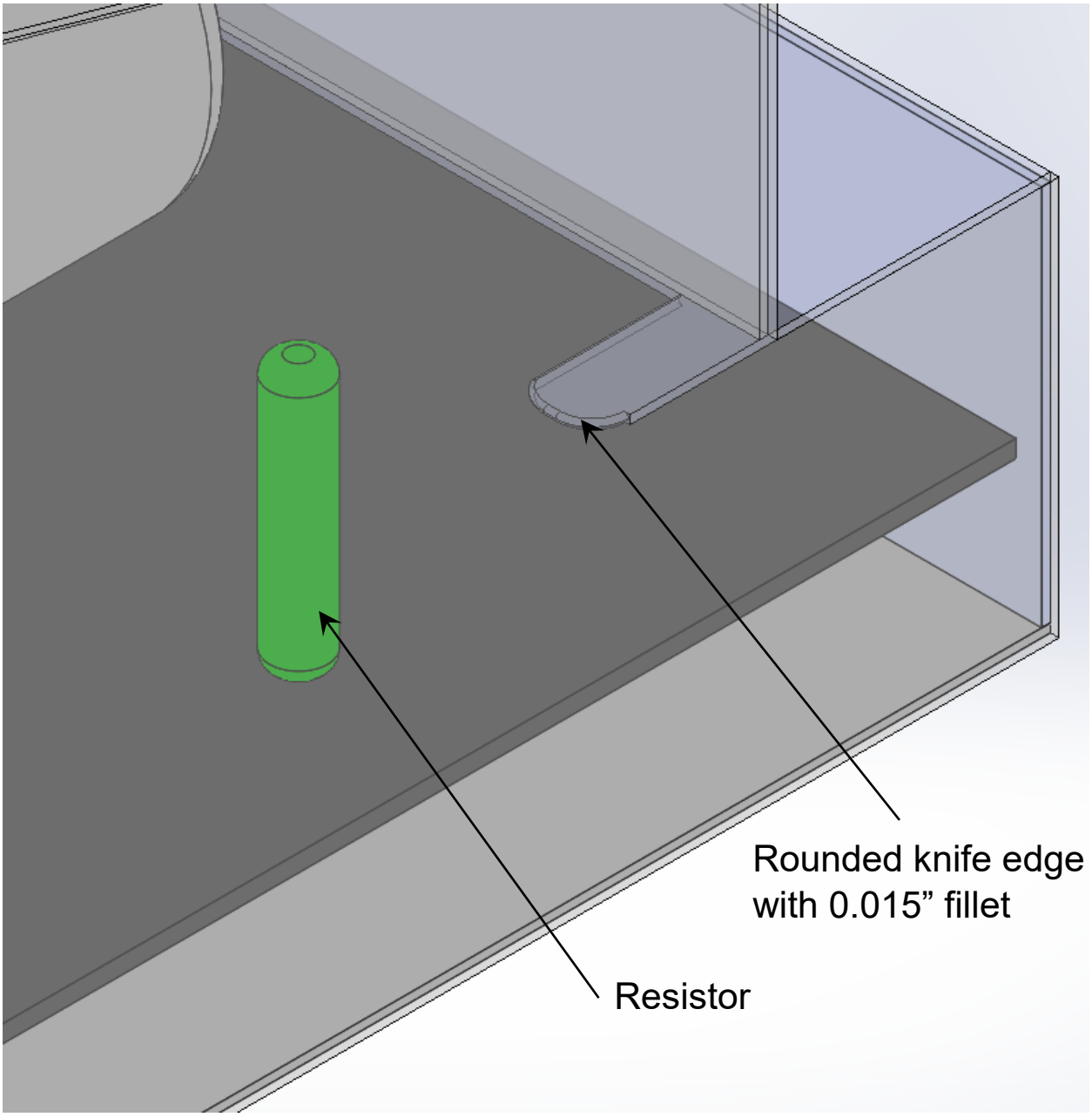

Figure 5

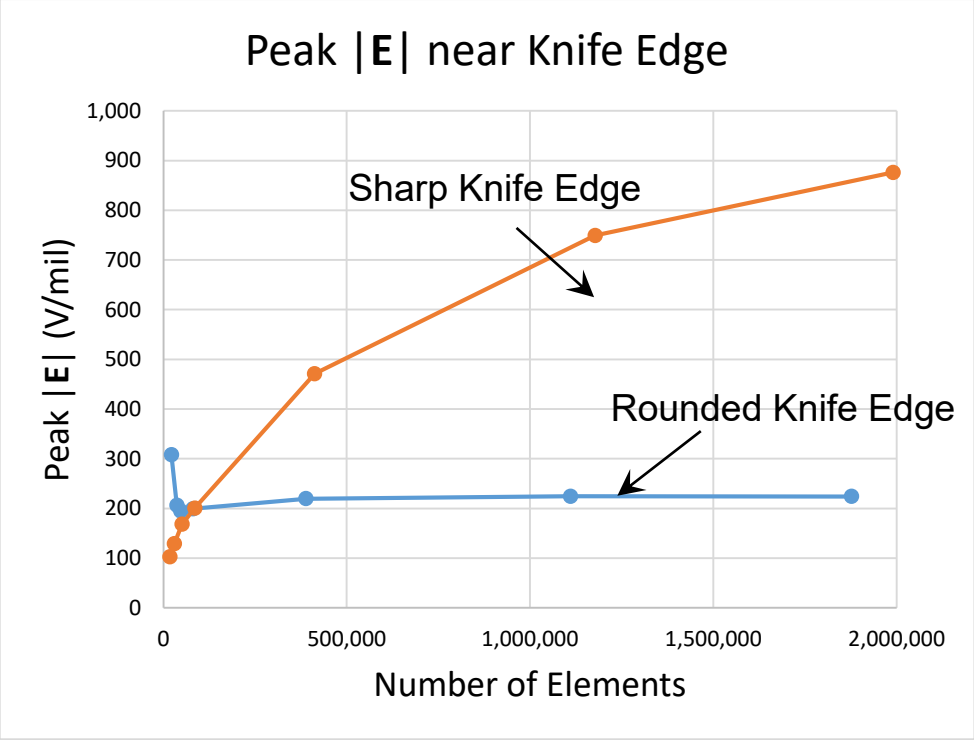
Peak |E| near Knife Edge
Peak |E| (V/mil)
1,000
900
800
700
600
500
400
300
200
100
0
Sharp Knife Edge
Rounded Knife Edge
0
500,000
1,000,000
1,500,000
2,000,000
Number of Elements

Figure 6

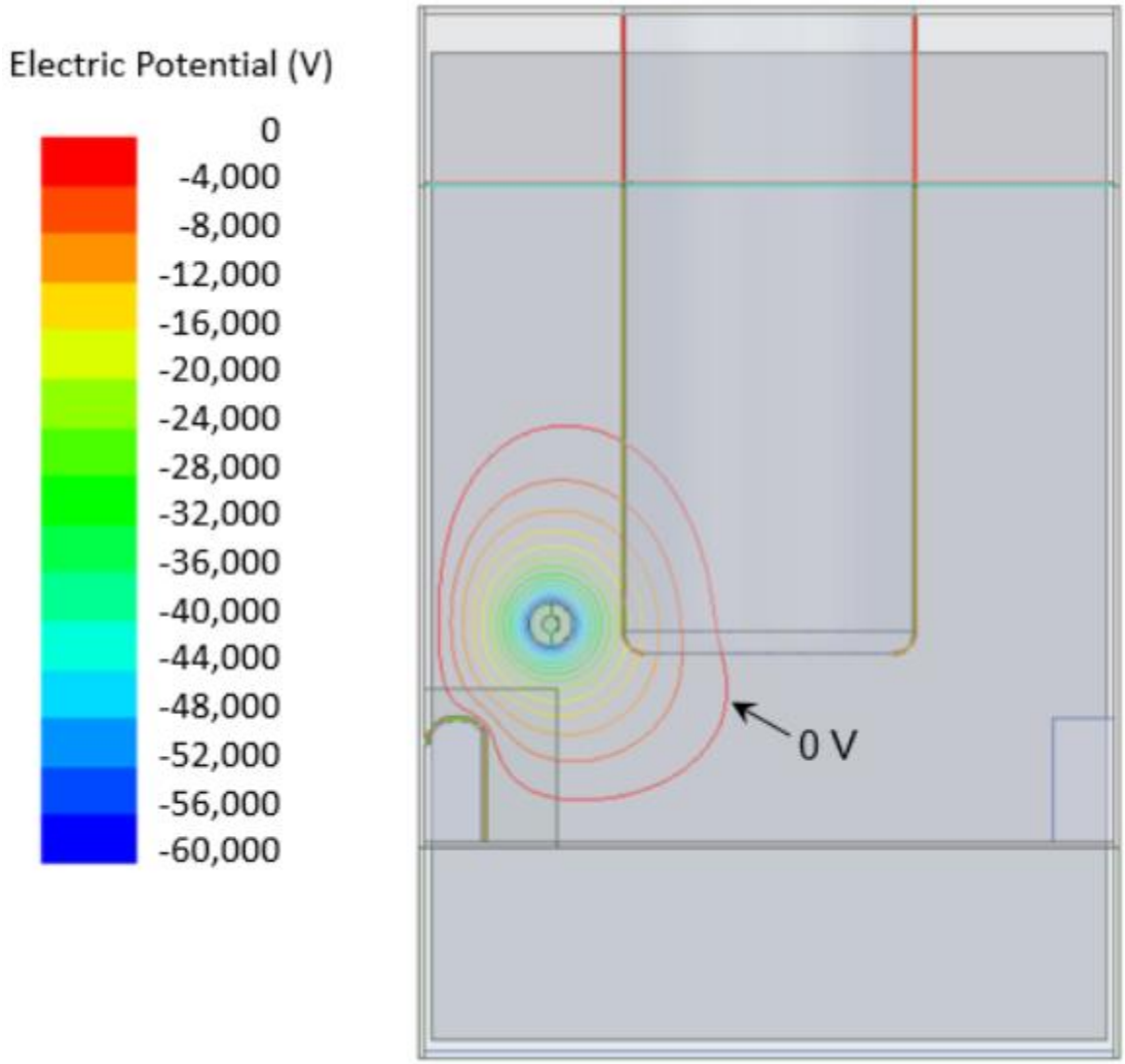

Figure 7a
Please use color for this figure in print.

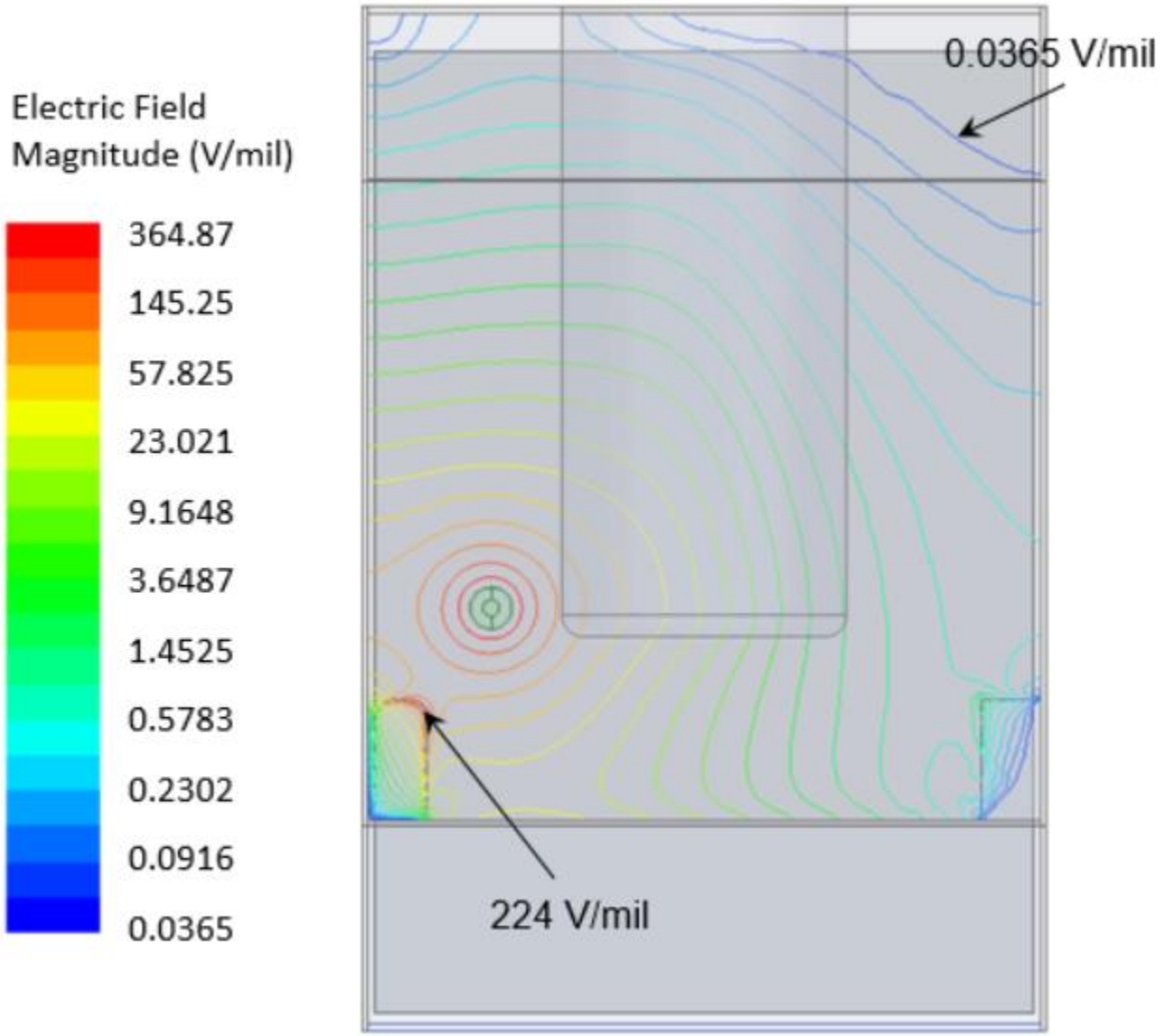

Figure 7b
Please use color for this figure in print.

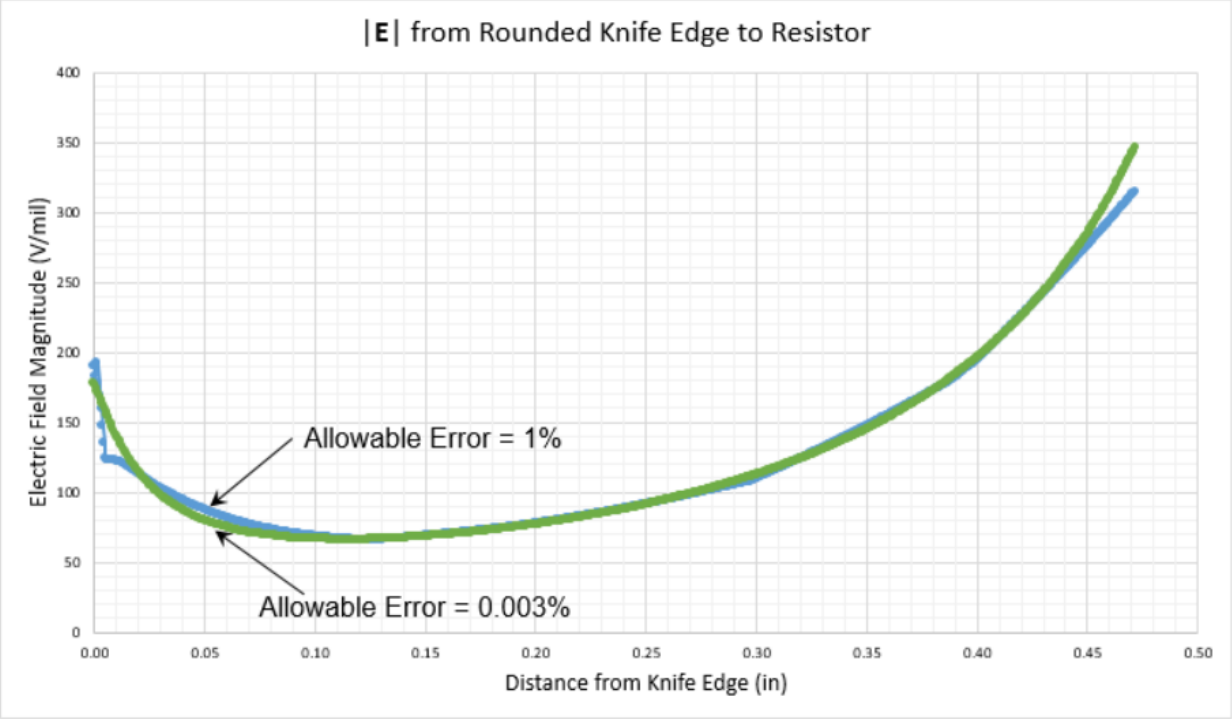
|E| from Rounded Knife Edge to Resistor
Electric Field Magnitude (V/mil)
Distance from Knife Edge (in)
Allowable Error = 1%
Allowable Error = 0.003%
400
350
300
250
200
150
100
50
0
0.00
0.05
0.10
0.15
0.20
0.25
0.30
0.35
0.40
0.45
0.50

Figure 7c